Original Research Article

Design and construction of a system for measuring carbon monoxide, hydrogen and methane concentrations in a co-current downdraft biomass gasifier

Abstract

Gasification is the process of producing combustible gases from solid materials such as coal, biomass or solid waste. Our laboratory of Space Physics and Energy has two experimental gasifiers producing synthetic gases whose natures and concentrations must be determined. To do this, lower-cost sensors were purchased and used for determining the concentration of carbon monoxide, hydrogen and methane in synthetic gas produced by a wood fired co-current downdraft gasifier. These sensors have a chemical sensing element based on a layer of tin dioxide (SnO2), whose resistivity is sensitive to nature of the gas between two sensing electrodes. This property gives these sensors a resistive electrical model whose measurand is the concentration of the input gas. This study is therefore the physical and mathematical modeling of these synthesis gas concentration sensors [c] = g (R) in order to allow their electronic exploitation with a microcontroller.

Keywords: Gasification, Modelling, Concentration, Carbon monoxide, Hydrogen, Methane

1. Introduction

Burkina Faso, efforts to reduce energy dependence (of populations and industries on fossil resources and wood) are being carried out through the development of renewable energy sources such as photovoltaic and thermal solar [1], [2]. To make our contribution to this concern, the Laboratory has therefore embarked on the construction of experimental gasifiers producing synthetic gases usable for the production of electricity. From May to august 2022, a first downdraft gasifier was designed and successfully tested two wood fired downdraft biomass in Burkina Faso [3], [4]. A second gasifier was designed and built from September to December 2022 in order to overcome design flaw that was found in the first gasifier during the testing's. The two gasifiers built are of the co-current type which are already used in industry from 100kW and above for their suitability, as well as their relative ease of manufacturing in developing countries. As a reminder, gasification is the process of producing combustible gases from solid materials such as coal, biomass or solid waste. However, faced with the diversity of combustion materials, one of the problems is to detect the nature of the gases produced as well as their concentrations with precision. The laboratory already has analyzers such as Testo 310, Bacharch (Fyrite Pro, Fyrite Intech 120, Monoxor III) with a measuring range of 1000 to 2000 ppm of carbon monoxide and which

saturate very quickly for higher concentrations.

Unfortunately, flue gas analyzers we have on hands are not built for continuous operation.
Because we out passed that manufacturer's restriction using the analyzers for 30 minutes or hours, we ended up damaging Oxygen and Carbon monoxide sensors. Replacing these sensors appeared out of reach for Bacharach® analyzers, because these sensors are relatively costly for underdeveloped countries as Burkina Faso and not suited for long run usage (maximum 5 minutes recommended by the manufacturers). Testo ® 310 XL analyzer doesn't didn't give leave us the possibility of replacing sensors. That analyzer should be sent back to a specialized manufacturer's maintenance center endowed with special tools for opening that hand held gas analyzer, replacing the bad sensors and recalibrating these. Therefore, we had no choice than looking for other solutions.
As said by Yulin Kong et al. [5]: "SnO2 has been extensively used in the detection of various gases. As a gas sensing material, SnO2 has excellent physical-chemical properties, high reliability, and short adsorption-desorption time". We also found in the literature that other authors were already using cheap gas monitoring sensors for industrial applications [6], [7], [8]. We also found that a microcontroller can be used to acquire data from numerous sensors, compute several mathematical functions and display these values [9], [10], [11]. This is why we anticipated that the combination of these gas sensors with a microcontroller would constitute a cost-effective replacement solution for monitoring gas concentrations in our biomass gasifiers and decided to build an experimental prototype system for measuring these gases, in particular carbon monoxide, hydrogen and methane.

2. Materials and methods

2.1 Experimental setup

The gasifier used in this work is composed of several functional units:

- The reactor
- The cyclone
- The condenser
- The filter

Figure 1 bellow shows the overview of these different parts. MQ gas sensors are located on a sampling box that draw small amount of synthetic gas cleaned of tar and water vapor by the cyclone separator, the condenser and the filter.

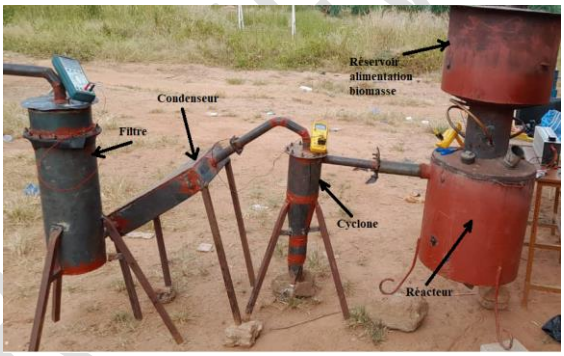

Figure 1 : Experimental setup

2.2 Methods

The main gases whose concentrations we want to detect and measure are: H_2, CO and CH_4. the respective sensors are: MQ-8, MQ-7, MQ-4.

2.2.1 Chemical behavour of MQ gas sensors

The basic chemical element of MQ gas sensors is a tin dioxide (SnO2) layer. From an electrical point of view, a perfect SnO2 crystal exhibits insulating behavior, due to its wide bandgap. Depending on the purity of the material, we note in the literature a large dispersion of the experimental values of the bandgap which varies between 2.25 to 4.3 eV [12]. On the basis of the results obtained by Jacquemin [13], we can consider that the band gap is direct and that the value of this band gap at room temperature varies between 3.5 to 4 eV. At the opposite, the real crystal has a semiconductor character. This behavior results from deviations from stoichiometry and is closely linked to the presence of oxygen vacancies leading to the presence of donor-type energy levels inside the bandgap [14].

2.2.2 Operating principle

The electrical properties of tin oxide layers are influenced by the gaseous chemical environment in contact with the layer. Thus, the absorption by physisorption or chemisorption of chemical species on the surface of the layer modifies its conductivity by a modification of the electronic states of the semiconductor by movement of electrons from the valence band towards the conduction band. This process is done in three steps [12]. Firstly, the layer is brought into contact with air and the adsorption of dioxygen molecules causes their dissociation and ionization in O- form (the most stable species at high temperature) by tearing off an electron from the band. conduction of the layer. Secondly, the reducing gas molecules, to be detected, react on the surface with the anions releasing an electron towards the conduction layer of the oxide and varying its electrical conductivity depending on the number of active oxidation sites and the number of gas molecules chemisorbed on the surface. Thirdly, following the cessation of the introduction of the gas, the oxygen present in the atmosphere adsorbs again on the surface of the oxide, returning to the equilibrium state established during the first process. However, this return to the equilibrium state assumes the absence of phenomena of poisoning of the sites by secondary molecules resulting from oxidation reactions. [14]

Given the above, the resistivity of the tin oxide layer varies depending on the concentration of environmental gases. We can model it by a variable resistance depending on the concentrations as shown on Figure 2 below.

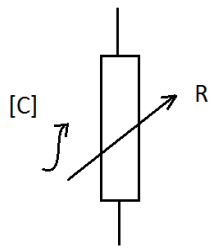

Figure 2 : Electrical model of a MQ gas sensor

2.2.3 Presentation of the sensors

The following Figure 3 is the representation of a gas MQ sensors.

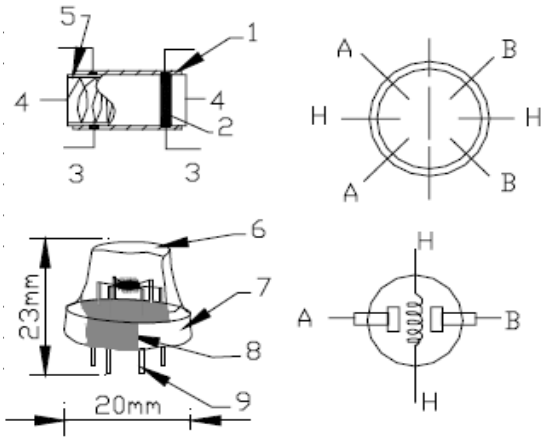

Figure 3 :MQ gas sensors structure

Each SnO_2 sensor is composed of the elements in *Table 1* below:

Table 1 : Constitutes of a gas sensor

	Parts	Materials
1	Gas sensing layer	SnO2
2	Electrode	Au
3	Electrode line	Pt
4	Heater coil	Ni-Cr alloy
5	Tubular ceramic	Al2O3
6	Anti-explosion network	Stainless steel gauze (SUS313 100-mesh
7	Clamp ring	Bakelite
8	Tube pin	Copper plating Ni

2.3 Mathematical model of the sensors

Depending on the type of sensor, the manufacturer has provided a standard catalog of correlation curves that we will use.

Curves $\log\left(\frac{R_S}{R_0}\right) = f([C]_{(ppm)})$

are plotted on a logarithmic scale and are linear. By changing variables

$Y = \log\left(\frac{R_S}{R_0}\right)$ and $X = log\ ([C]_{(ppm)})$,

theses equation becomes: $Y = A * X + B$.

Using the coordinates of two points

(X_1, Y_1) and (X_2, Y_2),

Wet get A and B :

$A = \frac{Y_1 - Y_2}{X_1 - X_2}$ and $B = Y_2 - \left(\frac{Y_1 - Y_2}{X_1 - X_2}\right) * X_2$

Subsequently, we will use the calibration curves provided in the technical datasheets to determine the coefficients A and B for each sensor according to the type of gas to be detected.

As said by "SnO_2 based MOS gas sensors are most popular for sensing a wide range of gases. Selection of a gas sensing material is crucial due to the fact that selectivity is an important characteristic for designing efficient gas sensing devices" [15]. We will therefore select the appropriate sensor for each gas we are willing to sense in paragraphs bellow.

2.3.1 Dihydrogen and derivatives

These gases are detected by the MQ8 sensor.

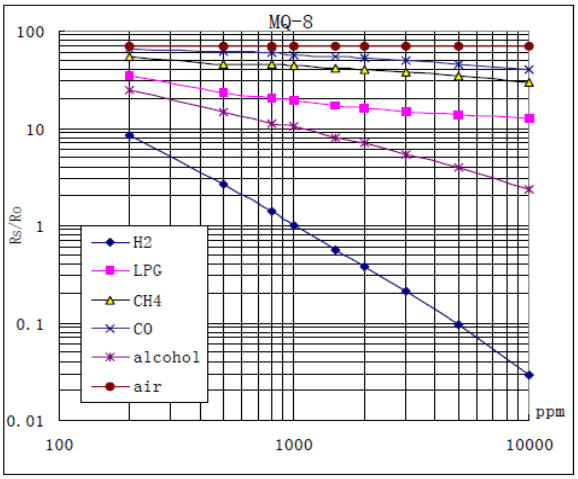

Figure 4 : MQ-8 sensitivity to different gases

As we can see on Figure 4 above: the sensitivity of MQ-8 sensor varies depending on the gas it detects. Hydrogen has the highest variation slope, then come alcohol with a smaller slop variation. Liquefied Petroleum Gas, methane carbon monoxide has very small variation slopes, similar to that of the air. Therefore, we will use MQ-8 for measuring hydrogen concentration in flue gas.

In Table 2 below, we have calculated the parameters A and B above for hydrogen.

Table 2 : Calculated values of A and B for MQ-8

AIR	70	100	0	1,845
	70	1000		
CO	Y =log (RS/R0)	X= log (ppm)	A	B
	50	3000	-0,18534	2,343
	40	10000		
CH4	Y =log (RS/R0)	X= log (ppm)	A	B
	40	2000	**-0,17875**	**2,1921**
	30	10000		
LPG	Y =log (RS/R0)		A	B
	20	800	-0,1570	1,7568
	15	5000		
ALCOL	Y =log (RS/R0)	X= log (ppm)	A	B
	4	5000	-0,61074	2,8612
	7	2000		
H2	Y =log (RS/R0)	X= log (ppm)		
	1	1000	A	B
	0,03	10000	-1,5229	4,5686

AIR

$$\log\left(\frac{R_S}{R_0}\right) = 1{,}8451 \leftrightarrow \frac{R_S}{R_0} = 10^{(1{,}8451)} = 70$$

H2

$$\log\left(\frac{R_S}{R_0}\right) = -1{,}5228 * \log(x) + 4{,}5686$$
$$= A * \log(x) + B$$

2.3.2 Dihydrogen carbon monoxide and others

These gases are detected with MQ-7 sensor with sensitivity characteristics reported on Figure 5 below. We can see there that hydrogen has the highest slop variation followed by carbon monoxide. Furthermore, the two curves are almost parallels. Therefore, in the case of gasification where carbon monoxide and hydrogen are the main components, ways should be found to determine separate concentration of either hydrogen or carbon monoxide and deduce concentration of the other.

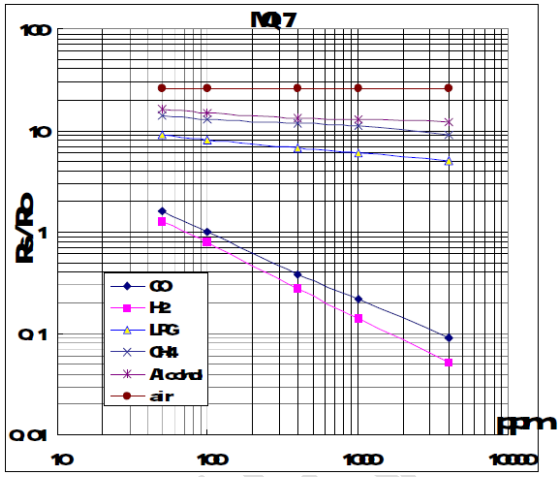

Figure 5 : MQ-7 sensitivity characteristics

Parameters A and B for MQ-7 are calculated in Table 3 : Parameters A and B calculation for MQ-7 below.

Only equation for CO is given on Table 3. H2 will be calculated from MQ-8 and deduced from MQ-7. For example, if MQ-8 reads a concentration [H_2] of hydrogen and MQ-7 reads concentration [H_2 + CO], we will calculate concentration [CO] as MQ-7 reading minus MQ-8 reading.

2.3.3 Methane and derivatives.

These gases are detected with MQ-4 sensor. Sensitivity characteristics of MQ-4 sensor is given on Figure 6 below:

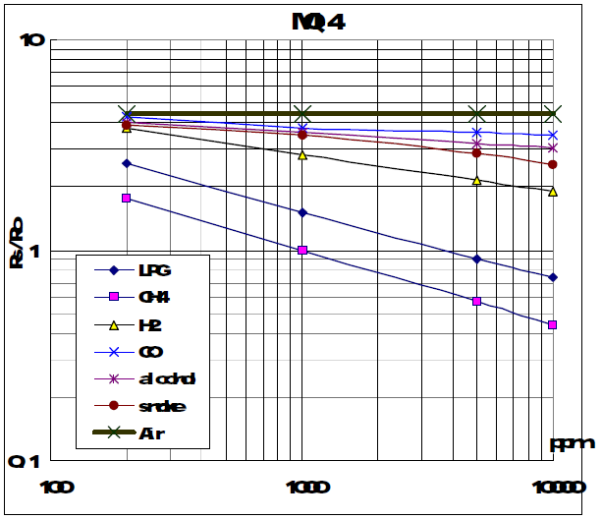

Figure 6 : Sensitivity characteristics of MQ-7

Table 3 : Parameters A and B calculation for MQ-7

Name of gas	Y =log (RS/R0)	X= log (ppm)	A	B
AIR	26	50	0	1,4150
	26	4000		
Alcohool	Y =log (RS/R0)	X= log (ppm)	A	B
	17	50	-0,06122	1,3345
	13	4000		
CH4	Y =log (RS/R0)	X= log (ppm)	A	B
	15	50	**-0,11657**	**1,3741**
	9	4000		
LPG	Y =log (RS/R0)	X= log (ppm)	A	B
	9	50	-0,13414	1,1821
	5	4000		
CO	Y =log (RS/R0)	X= log (ppm)	A	B
	1	100	-0,65276	1,3055
	0,09	4000		
H2	Y =log (RS/R0)	X= log (ppm)	A	B
	0,8	100	-2,0588	4,0207
	0,02	600		

AIR

$$\log\left(\frac{R_S}{R_0}\right) = 1{,}415 \leftrightarrow \frac{R_S}{R_0} = 10^{(1{,}4149)} = 26$$

CO

$$\log\left(\frac{R_S}{R_0}\right) = -0{,}6527 * \log(x) + 1{,}3055$$
$$= \mathrm{A} * \log(x) + B$$

As we can see, methane has the highest variation slop on MQ-4. It is followed by LPG. We will therefore use this sensor for detecting methane in produced gases.

2.3.4 Putting these gases sensors together

In case of gasification, we seek to produce mainly carbon monoxide and hydrogen, plus sometime methane.

The stoechiometric combustion of wood in air containing 21% of oxygen and 79% of nitrogen is the following equation:

$$\boldsymbol{C_6H_{12}O_5 + 6.5(O_2 + 4.77N_2) \xrightarrow{yields} 6H_2O + 6CO_2 + 31N_2} \quad (1)$$

When oxygen is not supplied in sufficient quantity, CO is produced in lieu and place of CO_2. Also, water vapor is engaged in the so-called water-gas shift reaction that produce hydrogen as a reaction between carbon dioxide and water vapor according equation 2 to below:

$$CO + H_2O \rightleftharpoons CO_2 + H_2 \quad (2)$$

Consequently, we have mixture of CO, H_2, CH_4, CO_2 and N_2 from the gasification of biomass.

Knowing the concentrations of each of these gases thank to MQ sensors will help us monitor the gasification process.

These gases concentration will be calculated with a microcontroller as a computer under the Microchip Integrated Development Environment (IDE) named MPLAB IDE v8.80.

3. Results and discussion

3.1 Calibration of the MQ gas sensors

Calibration of MQ gases sensors mainly consist in the determination of resistance Rs. For a concentration x given in ppm, we obtain an electrical resistance Rs at the sensor output through the following properties:

3.1.1. Mathematical equations for using gas sensors

Through the calibration curves, we know that:

$$\log\left(\frac{R_S}{R_0}\right) = A * \log(x) + B$$

If we note x the gas concentration in ppm, A and B the constants depending on the type of sensor used, the we can deduce:

$$x = 10^{\left(\frac{\log\left(\frac{R_S}{R_0}\right) - B}{A}\right)} \text{ or also}$$

$$\frac{R_S}{R_0} = 10^B * x^A \text{ or also}$$

$$x = \left(\frac{R_S}{R_0} * 10^{-B}\right)^{\frac{1}{A}}$$

We have summarized the values obtained for A and B in the two Table 4 and Table 5 below.

Table 4 :Parameter A values of the 3 gas sensors

MQ4 (CH4)	MQ7 (CO)	MQ8 (H2)
$-\mathbf{0},3072$	$-0,6527$	$-1,522$

Table 5 : Parameter B values of the 3 gas sensors

MQ4 (CH4)	MQ7 (CO)	MQ8 (H2)
0,921	1,3055	4,5686

Hence the following mathematical functional block in steady state for each sensor:

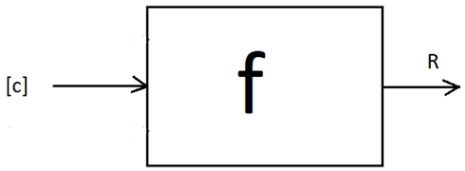

Figure 7 : Functional bloc of the sensors

[C]=x: concentration of the inlet gas.
R=Rs: output resistance.

f: the mathematical steady-state input-output correlation function.

3.1.2. Measurement range

The Table 6, Table 7 and Table 8 above represent the measurement ranges of the sensors.

Table 6 : H2 : MQ8

X= [C] (ppm)	100	10000
RS (kΩ)	10	60

Table 7 : CO : MQ-7

X= [C] (ppm)	10	10000
RS (kΩ)	2	20

Table 8 : CH4 : MQ-4

X= [C] (ppm)	100	10000
RS (kΩ)	10	60

3.1.3 Intrinsic sensitivity of the sensors

Intrinsic sensitivity of sensors for a variation of the output ΔR of the output, we can estimate the sensitivity through the input variation Δx.
It is equal to:

```
void gaz_processing (int8 canal_in)
 // gas concentrartion measurement fonction
 {
   float yy, xx,m, b0;
   int16 reste;
 // computing of correction coefficients
 // according to humidity
 k_rh_mq4= (val_humidity /-322.6)+ 1.10;
 k_rh_mq7= (val_humidity/-370.4)+ 1.09;
      if(canal_in==0)
      {
       k_r=1.1560;  //k_r= rl_mq7/r0_mq7;
       //k_g=0.889024;

       k_t_mq7=0.9408;  //à 34 degré celcius
       k_g= k_t_mq7  * k_rh_mq7;
       m=1.0/a_mq7;
       b0=20.2069143  ;//b0= pow(10,b_mq7);
        vs=vs_mq7;
      }

      if(canal_in==1)
      {
       k_r=1.1599;  //k_r= rl_mq4/r0_mq4;
       //k_g=0.887494;

        k_t_mq4=0.9578;
        k_g= k_t_mq4  * k_rh_mq4;
        m=-3.25520833;//m=1.0/a_mq4;
        b0=8.33681185  ;//b0= pow(10,b_mq7);
        vs=vs_mq4;
      }
```

$$\frac{\partial x}{\partial R_s} = \frac{1}{A} * \left(\frac{10^{-B}}{R_0}\right) * \left(\frac{R_s}{R_0} * 10^{-B}\right)^{\left(\frac{1-A}{A}\right)}$$

3.1.4 Implementation in MPLAB IDE

MPLAB IDE is written in C language. Equation from different sensors were derived for each sensor and we obtained results summarized below.

Figure 8 : Microchip MPLAB IDE logo

```
void main(void)  // main fonction
{

init_uc(); //microcontroleur initialisati

 while(1)  // loop
 {

  // mesurment of gas contration
    if(gaz_process==1)
     {
        gaz_process=0;
        acquisition ();
       integration(0);
      gaz_processing (0);
      integration(1);
      gaz_processing (1);
     }

      // measurement of humidity
      if(fin_hum)
     {
       fin_hum=0;
        humidity_processing ();
     }
```

Figure 9 : The main bloc of our program

As we can see on Figure 9 above, the main program is subdivided in six routines that do a given work. The most important of these is "gaz_processing ( )" that calculate the different concentrations of the gases as illustrated on Figure 10 below:

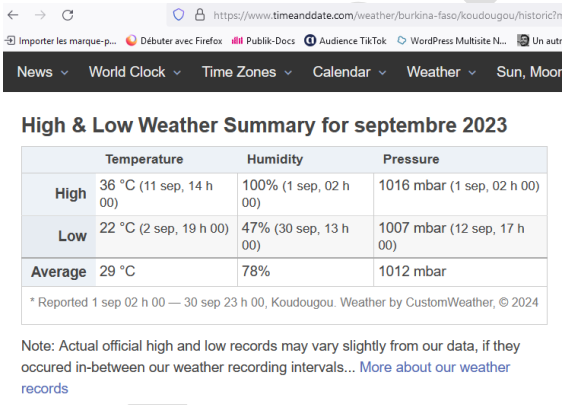

News | World Clock | Time Zones | Calendar | Weather | Sun, Moon

High & Low Weather Summary for septembre 2023

	Temperature	Humidity	Pressure
High	36 °C (11 sep, 14 h 00)	100% (1 sep, 02 h 00)	1016 mbar (1 sep, 02 h 00)
Low	22 °C (2 sep, 19 h 00)	47% (30 sep, 13 h 00)	1007 mbar (12 sep, 17 h 00)
Average	29 °C	78%	1012 mbar

* Reported 1 sep 02 h 00 — 30 sep 23 h 00, Koudougou. Weather by CustomWeather, © 2024

Note: Actual official high and low records may vary slightly from our data, if they occured in-between our weather recording intervals... More about our weather records

Figure 10 : The gases concentrations calculation function of the program

3.2 Electronic prototype

From the electronic diagrams, we were able to create some prototype power supply and conditioning boards (and). The measurement cards are made with Pic-kit cards from Microchip and Arduino uno.

The measurement system was fabricated with prototyping board and assembled together. The power supply board provides 5V, +8V and -8V voltages to the sensors and measurement amplifiers. as seen below:

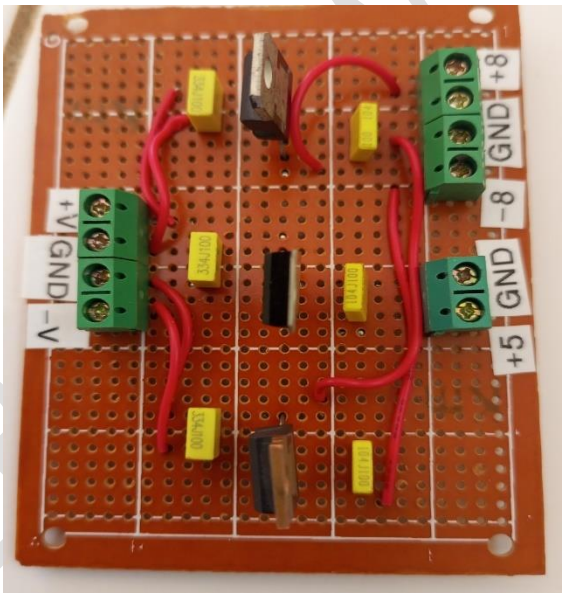

Figure 11 : Main power module

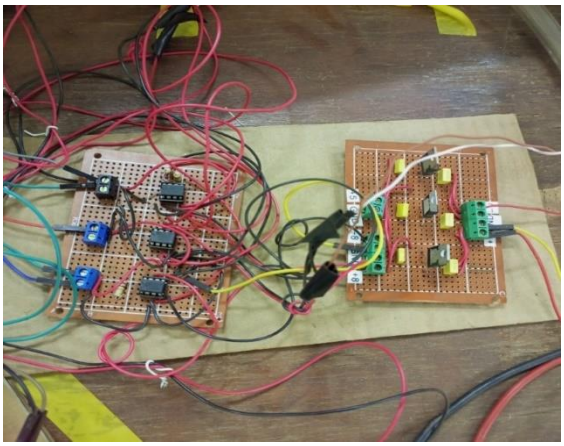

Figure 12 : Treatment and power supply boards

3.4 Tests results

On September 23, 2023, we carried out gasification measurement tests and obtained

CH4 concentration values = 310 ppm; CH4=10ppm; RH= 72%. Figure 13 represents a local display on an LCD screen of the gasification parameters obtained during the test.

These values were lesser than those we go from previous experiments in nearly similar experimental conditions: waste weigh, weather, etc.

Figure 13 : Test results on LCD display

These measurement results show low production of combustible gas. The air-dried wood used did not seem to have any problems and it had not rained in the 2 days preceding our handling. At that time, the oxygen concentration measurement module was not yet ready and we did not understand the reason for the failure of our manipulation. On November 1, 2023 at 5 p.m., we then took measurements of the humidity level of the ambient air. There we found 51%. On January 10, 2024, the indicated humidity level was 8%. We then looked for the causes of these differences in values and consulted the history of the weather in Koudougou. So for September 23, 2023, the following screenshot shows that the weather forecast indicated between 65 and 75% air humidity:

Figure 14 : Weather in Koudougou during September 2023

Conclusion therefore made that our gas measurement system is working as intended.

4. Conclusion

Through this study, we have highlighted the operation of gas concentration sensors made by Hanwey Corp. The test body of these sensors is a layer of tin dioxide (SnO2) whose resistivity is sensitive to contact gases and varies according to their concentration. The electrical model of these sensors is a resistance whose measurand is the concentration of the gas in contact. Thus, we were able to find the first physico-mathematical model of the CO, H2, CH4 gas sensors of our experimental gasifier. An electronic prototype was built and we have successfully measured CO and CH_4 concentrations together with relative humidity. The same method is applicable for H_2. However, these sensors are very sensitive to the temperature and humidity of the gases measured. These auxiliary parameters will be the subject of a study which will make it possible to find the real physical and mathematical model allowing judicious exploitation of these sensors.

5. REFERENCES

1 Joan Nyika, Adeolu Adesoji Adediran, Adeniyi Olayanju, Olanrewaju Seun Adesina and Francis Odikpo Edoziuno, The Potential of Biomass in Africa and the Debate on its Carbon Neutrality, Biotechnological Applications of Biomass, DOI: 10.5772/intechopen.93615, 2020

2 Sustainable Energy for All, [Burkina Faso]: Rapid assessment and gap analysis, pp. 1-2, https://www.seforall.org/sites/default/files/

Burkina_Faso_RAGA_FR_Released.pdf, Accessed 26 septembre 2023. French.

3 Nzihou Jean Fidele, Hamidou Salou, Imbga Kossi, Segda Bila Gerard, Ouattara Frederic, Tiemtore Hamadou, Electrical Power Generation from Heat Recovered at the throat of a Downdraft Biomass Gasifier, American Journal of Science, Engineering and Technology, 2023; 8(3) : 133-140, http://www.sciencepublishinggroup.com/j/ajset
doi: 10.11648/j.ajset.20230803.12, ISSN: 2578-8345 (Print); ISSN: 2578-8353 (Online)

4 Nzihou Jean Fidele, Hamidou Salou, Segda Bila Gerard, Ouattara Frederic and Compaore Hamidou, Effects of a Cyclone Dimensions on Quality of Syngas Produced with a Wood-fired Biomass Gasifier, Journal of Energy Research and Reviews, Article number JENRR.107030, ISSN: 2581-8368, Volume 15, Issue 3, Page 1-14, 2023

5 Yulin Kong, Yuxiu Li, Xiuxiu Cui, Linfeng Su, Dian Ma, Tingrun Lai, Lijia Yao, Xuechun Xiao, Yude Wang, SnO2 nanostructured materials used as gas sensors for the detection of hazardous and flammable gases: A review, Nano Materials Science, Volume 4, Issue 4, 2022, Pages 339-350, ISSN 2589-9651, https://doi.org/10.1016/j.nanoms.2021.05.006. 2022

6 I Kadek NuaryTrisnawan, Agung Nugroho Jati, Novera Istiqomah, Isro Wasisto, Detection of Gas Leaks Using The MQ-2 Gas Sensor on the Autonomous Mobile Sensor,

7 Nisal Kobbekaduwa, Pahan Oruthota and W.R. de Mel, Calibration and Implementation of Heat Cycle Requirement of MQ-7 Semiconductor Sensor for Detection of Carbon Monoxide Concentrations, Advances in Technology. 2021, 1(2), 377-392

8 Sohibun, I Daruwati, R G Hatika and D Mardiansyah, MQ-2 Gas Sensor using Micro Controller Arduino Uno for LPG Leakage with Short Message Service as a Media Information, URICSE 2021, Journal of Physics: Conference Series, (2021) 012068 IOP Publishing, doi:10.1088/1742-6596/2049/1/012068

8 Abubakar Yakub Nasir1, U. I. Bature2, N. M. Tahir3, A. Y. Babawuro4, Adoyi Boniface5 A. M. Hassan, Arduino based gas leakage control and temperature monitoring system, International Journal of Informatics and Communication Technology (IJ-ICT), Vol.9, No.3, December 2020, pp. 171-178, ISSN : 2252-8776, DOI : 10.11591/ijict.v9i3.pp171-178 Journal homepage: http://ijict.iaescore.com, 2020

10 Huan Hui Yan, Yusnita Rahayu, Design and Development of Gas Leakage Monitoring System using Arduino and ZigBee, Proceeding of International Conference on Electrical Engineering, Computer Science and Informatics (EECSI 2014), Yogyakarta, Indonesia, 20-21 August 2014

11 L Dewi and Y Somantri, Wireless sensor network on lpg gas leak detection and automatic gas regulator system using Arduino, IOP Conf. Serie: Material Sciences Engineering, 384 012064, 2018

12 Laghrib Souad, Synthesis of Thin Films of: Sno 2, Sno2: In by Two Physical and Chemical Processes and Study of Their Characterization, PhD Thesis, Ferhat Abbas University, Algeria, 139 pages, 2018. French.

13 J. Jacquemin. Optical PROPERTIES OF Intrinsic SnO2 AND β-PbO2 neighborhood of the gap. Journal de Physique Colloques, 1974, 35 (C3), pp. C3-255-C3-260. 10.1051/jphyscol:1974337. jpa-00215585

14 Laghrib Souad, Hania Amardjia-Adnani, Dahir Abdi, Jean-Marc Pelletier, Development and study of thin layers of SnO2 obtained by evaporation under vacuum and annealed under oxygen, Revue des Energies Renouvelables Volume 10 N°3 (2007) 357–366, 2007. French.

15 Priyanka Kakoty and Manabendra Bhuyan, Sn02 based gas sensors: Why it is so popular?